

Supporting Information

An Efficient All-Visible Light-Activated Photoswitches Based on Diarylethenes and CdS Quantum Dots

*Kezhou Chen,^{a,b} Jiayi Liu,^{a,b} Joakim Andréasson,^c Bo Albinsson,^{*c} Tiegen Liu,^{*a,b} Lili Hou^{*a,b,c}*

Mr. K. Chen, Ms. J. Liu, Prof. T. Liu, Prof. L. Hou

a. School of Precision Instrument and Opto-Electronics Engineering, Tianjin University, Tianjin 300072, China

b. Key Laboratory of Opto-electronics Information Technology (Tianjin University), Tianjin 300072, China

Prof. J. Andréasson, Prof. B. Albinsson, Prof. L. Hou

c. Department of Chemistry and Chemical Engineering, Chalmers University of Technology, Gothenburg 412 96, Sweden

E-mail: (lilihou@tju.edu.cn, tgliu@tju.edu.cn, balb@chalmers.se)

1. Method

Chemicals

Cadmium oxide, sulfur powder, 1-octadecene, and dioxane were purchased from Sigma Aldrich. Oleic acid was purchased from Alfa Aesar. Analytical reagent grade toluene and acetone was purchased from BOHAI chemical. Aberchrome 670, ferrioxalate, sodium-acetate-trihydrate and o-phenanthroline were purchased from Meryer. Sulphuric acid was purchased from Yuanli CHEM. All the chemicals were used without further purification. CdS QDs and **DAE 1** were synthesized according to previously reports. [1, 2]

Sample preparation

All photophysical measurements were carried out in toluene or n-hexane using 5- and 10-mm path quartz cuvettes. The concentrations of CdS QDs were determined from absorption spectra using the molar extinction coefficient according to the empirical functions:[3]

$$D = (-6.6521 \times 10^{-8})\lambda^3 + (1.9557 \times 10^{-4})\lambda^2 - (9.2353 \times 10^{-2})\lambda + 13.29 \quad (1)$$

$$\varepsilon = 21536(D)^{2.3} \quad (2)$$

where λ is the excitonic peak in the UV-visible absorption spectra, D is the diameter of QDs and ε is the molar extinction coefficient at the absorption peak.

The covalent sample was prepared by extraction with hexane/acetonitrile three times and precipitated with acetone once in centrifuge (8000 RPM, 30 min).

The solid sample was prepared by soaking a piece of 1 cm×1 cm filter paper film into the solution for UV-visible absorption measurement, letting all the solvent slowly evaporate at 70 °C in the dark.

Characterizations

Transmission electron microscopy (TEM, Tecnai G2, the Netherlands) was used to confirm the morphology of CdS QDs. X-ray diffraction (XRD, SHIMADZU 6100) was used to confirm the crystallinity of CdS QDs. UV-visible absorption spectra were measured using a Cary 60 UV-vis-NIR spectrophotometer. Steady-state photoluminescence spectra were recorded on a Cary Eclipse fluorescence spectrophotometer. Fluorescence lifetime measurements were carried out using time-correlated single photon counting (TCSPC), which was excited by a 377 nm laser diode (PicoQuant) and recorded by an MCP-PMT detector (10 000 counts, 2048 channels). Fourier-transform Infrared (FTIR) spectra were acquired using KBr pellets on a Nicolet 6700 spectrometer.

Light irradiations

For absorption spectra and long-term irradiation stability measurements, 310 nm irradiation was performed using a UV analytic lamp (4.5 mW) and 405 nm irradiation (72 mW) was carried out by using a continuous-wave laser (MDL-III-405). Visible irradiation was carried out by using a continuous-wave laser (MDL-III-405) coupled with a neutral density (ND) filter to reduce the intensity and an LED light source (Zolix MLED 4-3) with 515 nm irradiation (12 mW) for quantum yields measurements.

Quantum yield and conversion of photocyclization reactions

Photocyclization quantum yields were determined by using ferrioxalate actinometry according to standard methods.^[4] Fresh potassium ferrioxalate solutions (0.006 M, 3 ml) were irradiated for 1-5 min. 0.2 ml of the irradiated solution is mixed with 0.2 ml phenanthroline solution (5 mg o-phenanthroline dissolved in 5 ml water) and 0.1 ml of buffer solution (340 mg sodium-acetate-trihydrate dissolved in 2.5 ml water). 1.5 ml of this solution are mixed with 0.9 ml of 1 N sulphuric acid and thereafter diluted to 25 ml (this yields a buffer solution at pH 3.5)) and subsequently diluted with water to 2 ml. The quantum flow of incident light was determined by ferrioxalate using equation 3:

$$I_0 = \frac{\Delta AV_1 V_3 N_l 10^{-3}}{\Delta t \phi_{405} \varepsilon_{510} L V_2} \#(3)$$

Where ΔA is the difference in absorbance at 510 nm, V_1 is the irradiated volume (3 ml), V_3 is the used volume for subsequent addition of phenanthroline buffer (0.2 ml), N_l is the Avogadro number, Δt is the irradiation time, ϕ_{405} is the quantum yield of ferrioxalate at the irradiated wavelength ($\phi_{405} = 1.14$), ε_{510} is the extinction coefficient of the complex ($\varepsilon_{510} = 1.11 \times 10^4 \text{ Lmol}^{-1} \text{ cm}^{-1}$). L is the optical path length of the cuvette (5 mm), V_2 is the volume used for UV-visible absorption measurements (2 ml).

Photocycloreversion quantum yields were determined by using aberchrome 670 actinometry. 0.4 ml of the irradiated solution is measured in 5-mm path quartz cuvette. The quantum flow of incident light was determined by aberchrome 670 using equation 4:

$$I_0 = \frac{\Delta AV}{\Delta t \phi_{515} \varepsilon_{520} L} \#(4)$$

Where ΔA is the difference in absorbance at 515 nm, V is the irradiated volume (3 ml), Δt is the irradiation time, ϕ_{515} is the quantum yield of aberchrome 670 at the irradiated wavelength ($\phi_{515} = 2.98$), ε_{520} is the extinction coefficient of aberchrome 670 ($\varepsilon_{520} = 5.4 \times 10^3 \text{ Lmol}^{-1} \text{ cm}^{-1}$). L is the optical path length of the cuvette (5 mm).

We used aberchrome 670 and ferrioxalate, respectively, as actinometers at 515 nm and 405 nm to determine photochemical quantum yields ^[5]. QY was calculated from the initial slope of the recorded A-t-profile using the following equation:^[6]

$$\phi = \frac{\Delta AV}{\Delta t \varepsilon L (1 - 10^{-A(t)}) I_0} \quad \#(5)$$

with I_0 the quantum flow, V the volume of cuvette, ΔA the difference in absorbance at the absorption peak of **c-DAE 1**, ε the molar absorption coefficient at the absorption peak of **c-DAE 1** ($\varepsilon = 8.5 \times 10^3 \text{ Lmol}^{-1}\text{cm}^{-1}$), L the path length of the irradiation cuvette, and ϕ the quantum yield.

The conversions of the DAEs under visible light irradiation were determined according to the UV-visible absorption spectra in Fig. 2a. The concentrations of **c-DAE 1** were calculated using the molar absorption coefficient at the peak maximum in the visible band. The conversion from **o-DAE 1** to **c-DAE 1** at the photostationary state (PSS) was reported as 90% upon 310 nm irradiation,^[7] and the molar absorption coefficient of **c-DAE 1** was determined to be $\varepsilon_{510} = 8.5 \times 10^3 \text{ Lmol}^{-1}\text{cm}^{-1}$ in toluene. The PSS upon 405 nm light irradiation were calculated using equation 6.

$$PSS = \frac{A_{cp}}{\varepsilon_{cp} L c} \quad \#(6)$$

where A_{cp} is the absorbance of the band peak of **c-DAE 1** at the PSS after visible light irradiation; ε_{cp} is the molar absorption coefficient of **c-DAE 1** at the peak absorption, i.e. $\varepsilon_{510} = 8.5 \times 10^3 \text{ Lmol}^{-1}\text{cm}^{-1}$ for **c-DAE 1**; L is the optical path of the cuvette (1 cm); c is the concentration of **o-DAE 1** in the mixed solution.

2. Characterization of CdS QDs

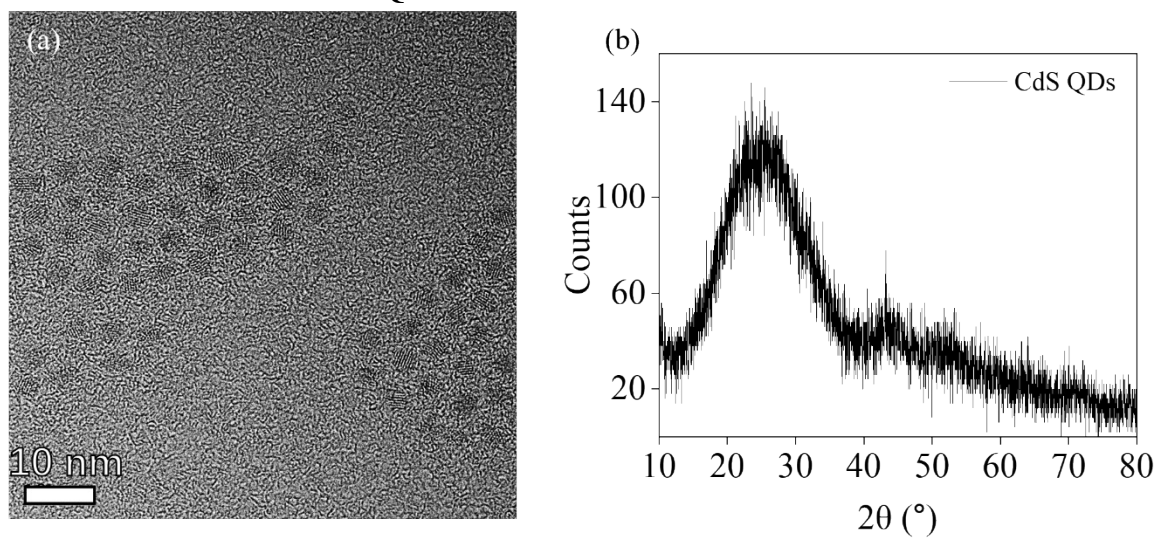


Figure S1. (a) TEM image of CdS QDs. (b) X-ray diffraction pattern of CdS QDs.

3. DAE 1 under visible light irradiation

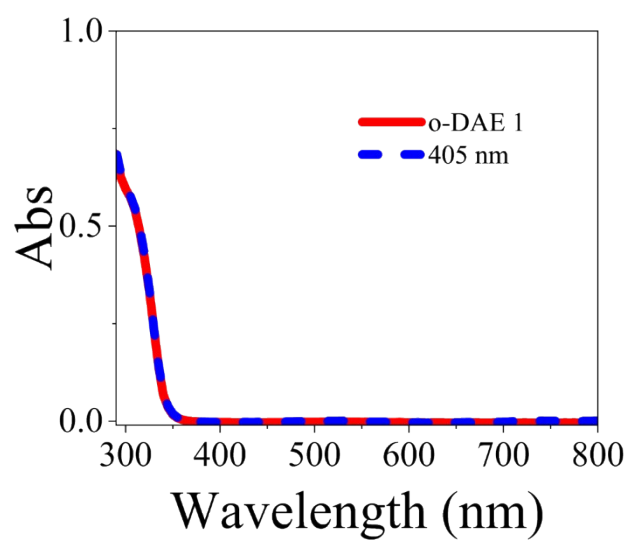


Figure S2. Absorption spectrum of **DAE 1** (50 μM) in toluene before (red-line) after 405 nm visible light irradiation (1 min, blue-dashed).

4. The ligands number of DAE 1/CdS QDs compounds by the method of ligand exchange

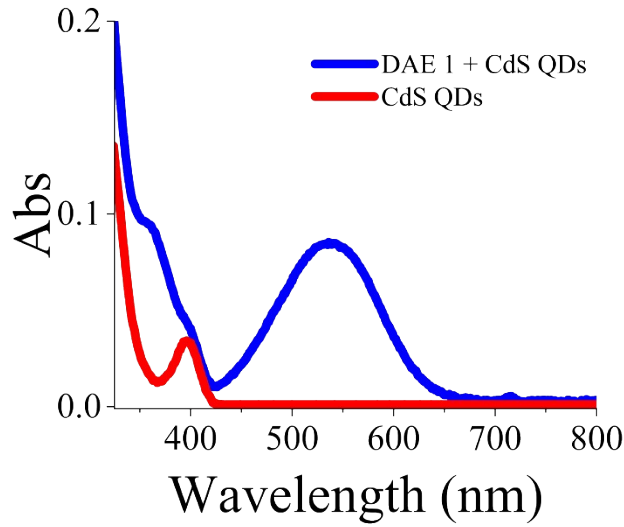


Figure S3. Absorption spectrum of CdS QDs and **DAE 1** anchored on CdS QDs by ligand exchange in toluene.

The covalent sample was initially comprised of prepared in the dark room

The ligands number of **DAE 1** molecules (m) per CdS QDs can be estimated from the absorption spectrum (Figure S2):

$$m = \frac{\frac{A_{DAE}}{\varepsilon_{DAE}}}{\frac{A_{CdS}}{\varepsilon_{CdS}}} \#(7)$$

where A_{DAE} is the absorbance of the band peak of c-**DAE 1** at the PSS after visible light irradiation; ε_{DAE} is the molar absorption coefficient of c-**DAE 1** at the peak absorption, i.e., $\varepsilon_{510} = 8.5 \times 10^3 \text{ Lmol}^{-1}\text{cm}^{-1}$ for c-**DAE 1**; A_{CdS} is the absorbance of the QDs at 405nm; ε_{CdS} is the molar absorption coefficient of CdS QDs at 405nm, $\varepsilon_{405} = 4.16 \times 10^5 \text{ Lmol}^{-1}\text{cm}^{-1}$. The number of covalent ligands of **DAE 1** anchored to the surface of one CdS QD was 9.52.

5. The PL quenching and PL lifetime of different relative concentrations

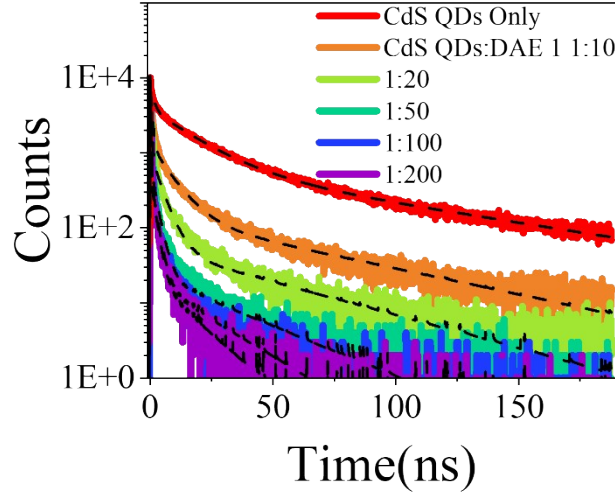


Figure S4. PL lifetime of the CdS QDs emission with and without the **DAE 1** (relative concentration of 10, 20, 50, 100 and 200) in toluene. The dashed lines indicate fits of three exponentials decay.

The time-resolved PL of CdS QDs exhibits complicated multi exponential decays. Herein, a three exponential decay was used to achieve a satisfactory fit:^[8]

$$I = I_0 \sum_{i=1}^3 A_i e^{\frac{-t}{\tau_i}} \quad \#(8)$$

where A_i and τ_i are the amplitude and lifetime of the i :th exponential component, respectively. The decays were deconvoluted using the instrument response function (IRF). The amplitude-weighted average lifetimes were calculated using equation 8

$$\langle \tau \rangle_{avg} = \frac{\sum_{i=1}^3 A_i \tau_i}{\sum_{i=1}^3 A_i} \quad \#(9)$$

The efficiency of the energy transfer, Φ_{ET} was estimated from PL lifetime quenching using equation 10

$$\Phi_{ET} = 1 - \frac{\langle \tau \rangle_{avg}}{\langle \tau_0 \rangle_{avg}} \quad \#(10)$$

To further investigate the quenching dynamics, we plot both the steady-state fluorescence intensity lifetime ratio F_0/F (Figure 3c) and τ_0/τ (Figure 3d) as a function of the **DAE 1** concentration for the bi-component system in a Stern–Volmer plot:

$$\frac{F_0}{F} = 1 + \tau_0 k_q c \quad (11)$$

$$\frac{\tau_0}{\tau} = 1 + \tau_0 k_q c \quad (11)$$

where τ_0 and τ are the average PL lifetime of CdS QDs without and with **DAE 1**, respectively, k_q is the quencher rate coefficient, and c is the concentration of the **DAE 1**.

Table S1. PL lifetime and energy transfer efficiency of CdS QDs mixed with **DAE 1**

CdS QDs: DAE 1	A ₁	τ_1 (ns)	A ₂	τ_2 (ns)	A ₃	τ_3 (ns)	$\langle\tau\rangle_{\text{avg}}$ (ns)	Φ_{ET}
CdS QDs only	0.5497	1.3	0.3722	16.4	0.0781	84.5	13.4	0
1:10	0.8544	0.6	0.1302	7.7	0.0155	62.5	2.5	81.2%
1:20	0.914	0.4	0.0814	4.2	0.0046	48.8	0.9	93.4%
1:50	0.9505	0.2	0.0478	2.4	0.0017	32.2	0.4	97.3%
1:100	0.962	0.2	0.0367	1.9	0.0013	22.1	0.3	98.0%
1:200	0.964	0.1	0.0345	1.8	0.0014	15.3	0.2	98.4%
1:400	0.962	0.1	0.0361	1.9	0.0017	13.2	0.2	98.4%

The PL quenching and PL lifetime of these solutions were measured at different relative concentrations. In comparison with the pure CdS QDs, the PL lifetime of **DAE 1**/CdS QDs are significantly reduced. $\langle\tau\rangle_{\text{avg}}$ (Table1) was reduced by 81% (13.4 \rightarrow 2.5 ns) when **DAE 1** was mixed with CdS QDs with relative concentration ratio of 10. Since o-**DAE 1** couldn't be transformed into c-**DAE 1** under 377 nm light irradiation, it demonstrates that the energy transfer occurs from CdS QDs to **DAE 1** and induces photoisomerization. The PL lifetime further reduced with a concomitant increase of energy transfer efficiency when the concentration of **DAE 1** increased in the solution.

6. Long-term stability of solid-state DAE 1 /CdS QDs sample



Figure S5. Images of a piece of paper prepared from CdS QDs and **DAE 1** solution, and its subsequent color (white and purple) change, upon visible light irradiation by simply varying the wavelength between 405 nm and 515 nm in a normal atmospheric environment after 5 days exposure to the air.

7. Reversibility of solid-state DAE 1 /CdS QDs sample

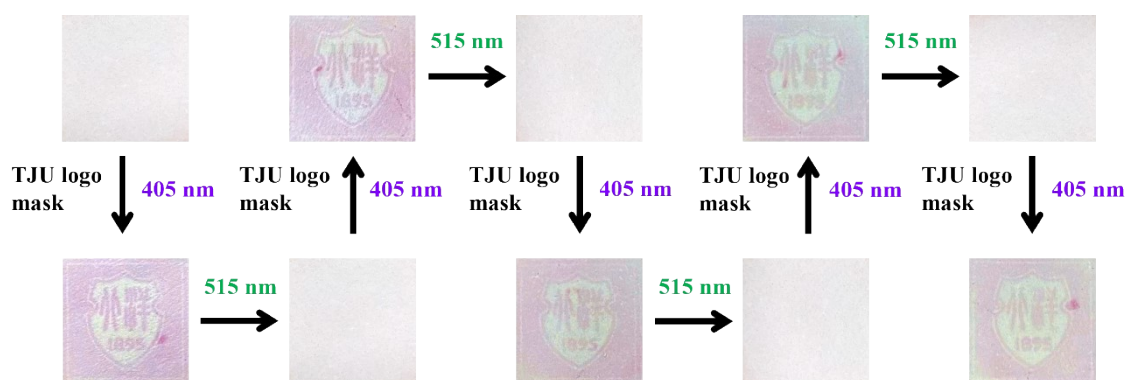


Figure S6. Images of a piece of paper prepared from CdS QDs and **DAE 1** solution, and reversibility of writing and erasing the same pattern of “TJU” logo, upon visible light irradiation by simply varying the wavelength between 405 nm and 515 nm over five cycles.

8. Reversibility and stability of DAE 1 /CdS QDs sample

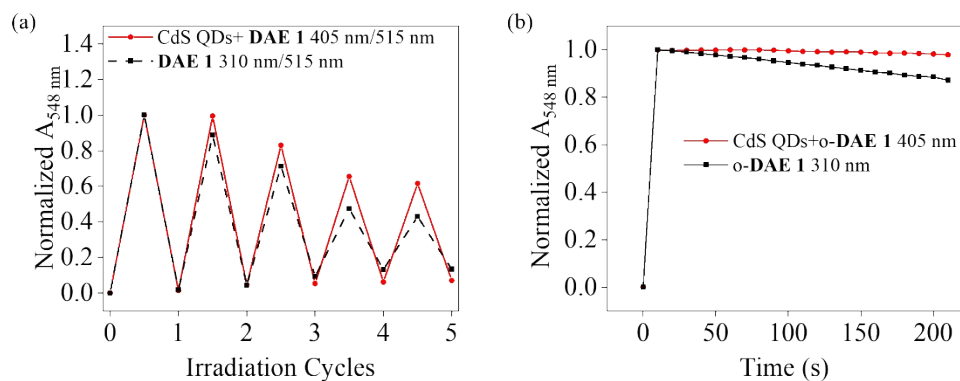


Figure S7. (a) Reversibility of the mixed solution as followed by the absorbance at 548 nm over five irradiation cycles of 405 nm and 515 nm light (red), and **DAE 1** only over five irradiation cycles of 310 nm and 515 nm (black). (b) Evolution of the absorbance at 548 nm of o-**DAE 1** in the mixture under 405 nm (red) and o-**DAE 1** only under 310 nm (black) light irradiation over time.

9. FTIR spectra of DAE 1 /CdS QDs sample

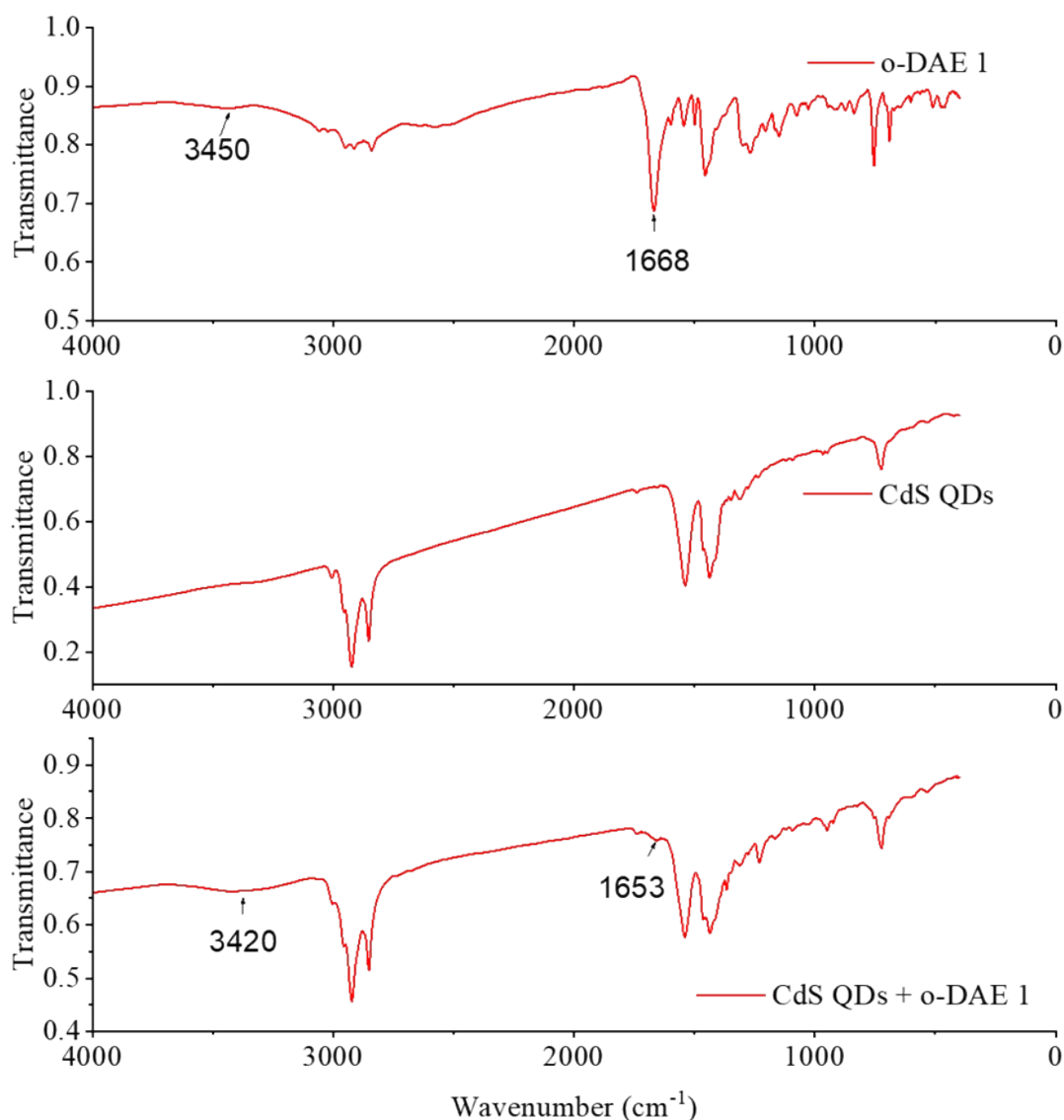


Figure S8. FTIR spectrum of **DAE 1**, pure CdS QDs and CdS QDs+ **DAE 1**.

FTIR spectroscopy was used to detect the carboxyl functional group on the surface of the CdS QDs when **DAE 1** anchoring on them. FTIR spectra of pure o-**DAE 1**, pure CdS QDs and CdS QDs + o-**DAE 1** were shown in Figure S6. The peak of 3450 cm^{-1} is ascribed to OH stretching of the $-\text{COOH}$ group and the stretching vibration of $-\text{C}=\text{O}$ is located at 1668 cm^{-1} . These two peaks can be clearly observed in the FTIR spectrum of o-**DAE 1** but absent in the that of CdS QDs. In the FTIR spectrum of the CdS QDs + o-**DAE 1** sample, the two peaks shifted to 3450 cm^{-1} and 1653 cm^{-1} , indicating surface anchoring to the CdS QDs.^[9, 10]

References

- [1] Z. Li, Y. Ji, R. Xie, S. Y. Grisham, X. Peng, *J. Am. Chem. Soc.*, **2011**, 133, 17248.
- [2] W. W. Yu, X. Peng, *Angew. Chem. Int. Ed.*, **2002**, 41, 2368.
- [3] W. W. Yu, L. Qu, W. Guo, X. Peng, *Chem. Mater.*, **2004**, 16, 560.
- [4] M. Montalti, S. L. Murov, *Handbook of photochemistry*, CRC/Taylor & Francis, Boca Raton **2006**.
- [5] A. P. Glaze, H. G. Heller, J. Whittall, *J. Chem. Soc., Perkin Trans. 2*, **1992**, 591.
- [6] K. Stranius, K. Borjesson, *Sci. Rep.*, **2017**, 7, 41145.
- [7] M. Herder, B. M. Schmidt, L. Grubert, M. Patzel, J. Schwarz, S. Hecht, *J. Am. Chem. Soc.*, **2015**, 137, 2738.
- [8] L. Hou, W. Larsson, S. Hecht, J. Andréasson, B. Albinsson, *J. Mater. Chem. C*, **2022**, 10, 15833.
- [9] G. A. Shandryuk, E. V. Matukhina, R. B. Vasil'ev, A. Rebrov, G. N. Bondarenko, A. S. Merekalov, A. M. Gas'kov, R. V. Talroze, *Macromolecules*, **2008**, 41, 2178.
- [10] D. H. Hu, H. M. Wu, J. G. Liang, H. Y. Han, *Spectrochim. Acta A Mol. Biomol. Spectrosc.*, **2008**, 69, 830.